JONRA

Journal of Nuclear Research and Applications

Research Paper

Vol. 3, No. 4, P 1-11, Autumn (2023)

Cited in: https://jonra.nstri.ir

Received: 20 June 2023, Revised: 17 September 2023, Accepted: 8 October 2023

Ab Initio Study of Mechanical and Vibrational Characteristics of Uranium Monoxide in Nuclear Reactor

M. H. Sahafi[1]*, E. Cholaki[2]

[1]*Department of Physics, Sharif University of Technology, P.O. Box 11155-9161, Tehran, Iran*
[2] *Department of Physics, Faculty of Science, Islamic Azad University of Kermanshah, Kermanshah, Iran*

ABSTRACT

By using density functional theory and the ab initio method for projector augmented wave pseudopotential parameterization, the mechanical and phonon properties of UO in the rock-salt phase have been systematically calculated. At null pressure and temperature, the obtained lattice constant is in good agreement with the experimental one. Mechanical stability is confirmed because the positive elastic constants meet the Born-Huang criteria. Mechanical properties including bulk modulus, shear modulus, and Young's modulus are evaluated using the Voigt-Reuss-Hill approximation. The value of Poisson's ratio (ν) is nearly 0.36, which shows that this compound has an ionic bond and interatomic forces within the crystal are central. The elasticity analysis of the Kleinman parameter reveals that bond bending is dominant within the substructure of UO. The vibrational density of states and phonon dispersion are investigated through the linear response approach. The results show the dynamical stability of crystalline structure due to the inexistence of virtual frequencies in dispersion relations.

Keywords: *Power Reactor; Nuclear Fuel; Density Functional Theory; Phonon Spectrum; Elastic Properties.*

1. Introductions

Actinides' unique properties have recently gained considerable attention among scholars [1]. The Uranium ion leads to anomalous characteristics in the chemical stability and structural and magnetic properties of Uranium alloys. This is owing to its trivalent state and the contentious treatment of 5*f* electrons in the valence layer. The 5*f* electrons exhibit localized behavior and undergo intense oscillations within the immobile region of the nucleons. Therefore, the elastic,mechanical, and phonon spectrum characteristics of rare earth composites are predominantly influenced by electron delocalization, as stated . In contemporary times, nuclear research professionals have proposed the concept of

*. *Corresponding Author name*: M. H. Sahafi
E-mail address: hosseinsahafi91@gmail.com

developing novel fuels constituted of uranium, with the aim of replacing traditional nuclear fuels in advanced reactors. The mixed oxide fuels constitute a promising option for technological deployment within the nuclear domain. The favorable attributes of uranium alloys, which include, low corrosion, low thermal expansion coefficient, high melting point, and high shock resistance [2], render them suitable for utilization as fuel pellets in the advanced fourth generation of nuclear reactors. In contemporary times, studies have been conducted on uranium compounds through theoretical and experimental methodologies, as evidenced by scholarly publications [3-10]. The comprehensive investigation of the electronic, dynamic, and thermal characteristics of U_3Si_2 alloy was carried out by Chattaraj et al. [8] through the use of density functional theory (DFT) and first-principles calculations. Wang et al. [9] have conducted a study that employs ab initio calculations based on the local density approximation to estimate high-pressure-induced structural phase transition alongside uranium dioxide's associated mechanical and thermodynamic properties. Chen [11] conducted a study on the mechanical and thermal properties of the *a*-$Na_3(U_{0.\ 84(2),}\ Na_{016(2)})O_4$ alloy, utilizing the quasi-harmonic Debye model and ab initio techniques. Mehmetoglu [12] has documented the constant-pressure molar capacity and thermal conductivity of UO_2 through the Debye-Einstein model, drawing on both semi-empirical and analytical approaches. Yamashita et al. [13] conducted an experimental investigation of the thermal expansion coefficient of mixed oxides of neptunium and uranium ceramics the X-ray diffraction. So far, UO's hardness, elastic coefficients, and mechanical properties, as a suitable candidate for fuel in advanced power plants, have not been extensively studied; hence, this issue motivated us to investigate these physical quantities.

The current investigation scrutinizes the elastic anisotropy, phonon spectrum, and mechanical characteristics of UO by means of density functional perturbation theory (DFPT) within the context of ab initio calculations. As delineated in Chapter 2, a thorough explication of the calculation methodology, encompassing pseudopotentials and computational code, will be provided. Chapter 3 outlines the applicable theoretical techniques for analyzingmechanical properties. The presentation of the findings, along with their analysis, will be discussed in the fourth chapter. The ultimate discussion and final outcome will be discussed in the concluding chapter, chapter five.

2. Computational Details

In order to derive an approximation for the energy of the lowest possible state of a given crystal lattice, the ab initio approach is employed, specifically utilizing the PAW pseudopotential methodology. The application of the Quantum ESPRESSO software [14], a computational package designed for band structure analysis, is utilized to calculate the Kohn-Sham relations. The self-consistent cycles employ the Perdew-Burke-Ernzerhof (PBE) functional, encompassing the exchange-correlation potential of the generalized gradient approximation, to characterizeelectron-ion interactions. The convergence thresholds for force and energy are set to 10^{-5}Ry and 10^{-4} Ry/bohr, respectively. The wave functions' energy distribution and corresponding energy threshold are selected as 0.05 Ry and 200 Ry, respectively, in accordance with established academic standards. By selecting these settings, the disparities among the self-consistent iterations are effectively limited to 10^{-4} eV/atom. The first

Brillouin zone is discretized into a 20×20×20 (*K-Point*) grid, encompassing highly symmetric directions, through the utilization of the Monkhorst-Pack technique [15]. A Marzari-Vanderbilt scheme [16] is then employed to integrate the 1BZ. The present study employs the linear response procedure in the framework of DFPT [17] to carry out the vibrational calculations. In this technique, critical insights concerning the dynamics of a crystal lattice can be obtained through the derivation of interatomic force constants and dynamical matrices. These parameters are determined using the nuclear geometry and electronic charge, and thus provide essential data pertaining to lattice dynamics. The present study utilizes the Broyden–Fletcher–Goldfarb–Shanno method [18] to examine the dynamics of molecules in order to achieve relaxation of the crystalline structure and minimize the forces attributable to Hellmann-Feynman. The phonon diagram for a 4×4×4 lattice at a particular q-point is determined by analyzing the phonon behavior at the irreducible points.

3. Theoretical Methods

3.1. Elastic/ Anisotropy Properties

The utilization of elastic coefficients can facilitate a comprehensive understanding of various aspects pertaining to polycrystals, including hardness, structural stability, dynamical characteristics, and mechanical behaviors. The aforementioned coefficients are instrumental in furnishing valuable insight pertaining to the exertion of operational forces in solids, as well as the material's ability to endure extrinsic and macroscopic stress. Cubic polycrystals possess three distinct elastic coefficients, C_{11}, C_{12}, and C_{13}, which are independent of each other.The methodology employed for the computation of these constants is the stress-strain approach, as documented in reference [19]. In this approach, a slight perturbation is introduced to the arrangement of crystalline planes, resulting in their deformation, thus generating a restorative stress that drives the system towards an equilibrium state. This process is outlined below:

$$\begin{pmatrix}\sigma_1\\ \sigma_2\\ \sigma_3\\ \tau_1\\ \tau_2\\ \tau_3\end{pmatrix} = \begin{pmatrix} C_{11} & C_{12} & C_{13} & 0 & 0 & 0 \\ & C_{22} & C_{23} & 0 & 0 & 0 \\ & & C_{33} & 0 & 0 & 0 \\ & & & C_{44} & 0 & 0 \\ & sym. & & & C_{55} & 0 \\ & & & & & C_{66} \end{pmatrix} \begin{pmatrix}\varepsilon_1\\ \varepsilon_2\\ \varepsilon_3\\ \gamma_1\\ \gamma_2\\ \gamma_3\end{pmatrix} \quad (1)$$

The present study utilizes mathematical notation to express the normal Eulerian strain, shear strain, normal stress, and shear stress as ε_i γ_i σ_i and τ_i, respectively. The first relation, commonly referred to as Hooke's Law, characterizes the attributes of the requisite forces that facilitate the expansion or contraction of an elastic medium. The crystalline structure experiences perturbation via a 3×3 symmetrical strain tensor having ±0.0075 and ±0.0025 components along the *xy*, *xz*, and *yz* planes. The stress tensor elements are determined via linear regression analysis of stress as a function of strain. The symmetrical nature of the lattice structure results in the reduction of elastic constants to 9 non-zero coefficients, specifically C_{11}, C_{22}, and C_{33}, which exhibit equality, in addition to C_{12}, C_{13}, and C_{23}, as well as C_{44}, C_{55}, and C_{66}. It is noteworthy that these coefficients remain independent of the Laue class. The evaluation of mechanical stability entails the substitution of the autonomous elastic coefficients in accordance with the Born-Huang criterion [20], as indicated below:

$$\begin{Bmatrix} C_{11} > 0; C_{44} > 0 \\ C_{11} - C_{12} > 0 \\ C_{11} + 2C_{12} > 0 \end{Bmatrix} \quad (2)$$

for calculating the elastic moduli [21], including the bulk modulus (B_H) and shear modulus (G_H)

Voigt-Reuss-Hill approximation is employed, as mentioned below:

$$\begin{Bmatrix} B_H = \frac{1}{2}(B_R + B_V) \\ G_H = \frac{1}{2}(G_R + G_V) \end{Bmatrix} \quad (3)$$

In simple words, the letters R and V are used to show the smallest and biggest numbers that measure and the strength of a material. These numbers are used to calculate an average strength for cubic materials, and are known as the Reuss and Voigt bounds.

$$\begin{Bmatrix} B_R = B_V = \frac{1}{3}(C_{11} + 2C_{12}) \\ G_R = \frac{5C_{44}(C_{11}-C_{12})}{4\,C_{44}+3(C_{11}-C_{12})} \\ G_V = \frac{1}{5}(C_{11} - C_{12} + 3C_{44}) \end{Bmatrix} \quad (4)$$

The Poisson's ratio (v) and Young's modulus (Y) are expressed through elastic coefficients as:

$$\begin{Bmatrix} Y = \frac{9B_H G_H}{3B_H + G_H} \\ Y = \frac{3B_H - Y}{6B_H} \end{Bmatrix} \quad (5)$$

Over the past few years, various techniques centered on elastic coefficients have been suggested for the evaluation of specific macroscopic characteristics, such as Vickers hardness. Within the scope of available techniques, a collection of empirical equations has been developed, which enables material stiffness determination.

$$\begin{Bmatrix} H_V^B = 0{,}0963\ B \\ H_V^G = 0{,}1475\ G \\ H_V^Y = 0{,}0608\ Y \end{Bmatrix} \quad (6)$$

The characterization of directional properties in materials is of paramount importance, with anisotropy being a critical feature in this regard. The following section elucidates the Zener anisotropy factor (A^z) and the elastic anisotropy, which is established through the universal index (A^U) [21]:

$$\begin{Bmatrix} A^Z = \frac{2C_{44}}{C_{11} - C_{12}} \\ A^U = 5\frac{G_V}{G_R} + \frac{B_V}{B_R} - 6 \end{Bmatrix} \quad (7)$$

The Lamés' coefficients (μ λ) and Kleinman parameter (ζ) are calculated as:

$$\begin{Bmatrix} \zeta = \frac{C_{11} + 8C_{12}}{7C_{11} + 2C_{12}} \\ \mu = \frac{Y}{2(1+v)} \\ \lambda = \frac{vY}{(1+v)(1-2v)} \end{Bmatrix} \quad (8)$$

The Debye temperature constitutes a crucial parameter in characterizing thermal enthalpy and volumetric expansion properties. Its estimation is accomplished via the application of the semi-empirical approach [22, 23]:

$$\begin{Bmatrix} \theta_D = \frac{h}{k}\left[\frac{3n}{4\pi}\left(\frac{N_A}{M}\rho\right)\right]^{1/3} v_m \\ v_m = \left[\frac{1}{3}\left(\frac{2}{v_s^3} + \frac{1}{v_B^3}\right)\right]^{-1/3} \\ v_l = \sqrt{\frac{B + \frac{4}{3}G}{\rho}} \\ v_s = \sqrt{\frac{G}{\rho}} \end{Bmatrix} \quad (9)$$

The present study employs technical nomenclature to denote distinct physical quantities. Specifically, the notations v_m, v_l, and v_s represent the average, compressional, and shear sound velocities, respectively. Besides, h and K_B denote the Plank and Boltzmann constants, respectively, while N_A represents Avogadro's number. Further, n stands for the number of atoms present within a

conventional unit cell, M signifies the molar mass, and ρ symbolizes density.

The determination of the melting point is achieved through the application of elastic coefficients [22, 24]:

$$T_m = 553 + 5{,}91C_{11} \pm 300\ \text{K} \quad (10)$$

4. Results and Discussion

4.1. Structural Properties

The process of Uranium monoxide crystal growth with a space group of Fm3m (No. 225) is the subject of academic inquiry. At ambient conditions of pressure and temperature, the primitive unit cell of a substance exhibits two disparate atoms that are not equivalent. The UO binary compound exhibits a face-centered-cubic geometric configuration, whereby the U and O atoms occupy the 4a and 4b Wyckoff positions, respectively, with their corresponding spatial coordinates being (0, 0, 0) and (0.5, 0.5, 0.5). The illustration depicted in Figure 1 portrays the structure of UO in its cubic form, specifically in the rock-salt phase. To optimize of the crystalline structure, it is necessary to minimize the total energy with consideration of volumetric modifications. Figure 2 illustrates the curve depicting energy variations with respect to the volume of the unit cell. The point of equilibrium, V_0, is reflected at the minimum of the curve. The special equation [25] is used to find some important parameters about the structure of a material. We found the size of the material when it is not being pushed or pulled (lattice parameter), how stiff it is (bulk modulus), and how that stiffness changes with pressure (a derivative of the bulk modulus). The investigation compiledthe obtained quantities and presented them in Table 1. The results have then been compared with the available empirical data [6]. The disparity between the obtained lattice constant and its experimental counterpart, approximating a 2% decrement,, becomes evident. This discrepancy may be attributed to the contrasting nature of the theoretical models employed and the experimental measurements. The degree of agreement between the aforementioned parameters and the empirical data serves as an indication of the validity and dependability of the computational methods employed in this study.

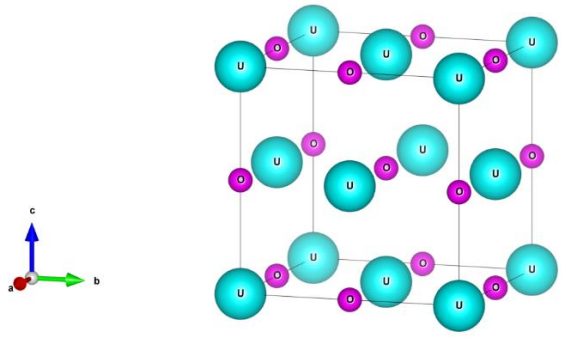

Fig. 1. The conventional unit cell of UO in NaCl-B1 phase.

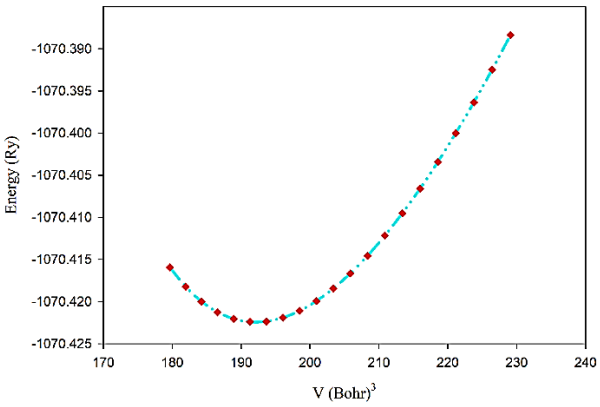

Fig. 2. The changes of total energy versus unit cell volume.

Table 1. Calculated the structural properties of uranium monoxide.

material	a_0(Å)		$B_0(GPa)$	B_0'
	This work	Exp	This work Theory	
UO	4.84	4.94[6]	200 198 [5]	4.91

4.2. Elastic and Mechanical Properties

The elastic constants [24] are crucial magnitudes that indicate a crystal's capacity to resist external

pressure applied to it. Elastic coefficients evaluate bonding characteristics, sound wave transmission, mechanical resilience, and pliability. Table 2 presents the second-order elastic coefficients attained under equilibrium conditions. All the elastic stiffness parameters demonstrate positivity and conform to the equations set forth in (2), indicating UO's mechanical stability. Table 2 presents the mechanical properties, which encompass the bulk modulus, shear modulus, Young's modulus, Poisson's ratio, and Pugh's criteria (*B/G*). The bulk modulus (*B*) is a fundamental physical parameter used to assess the compressibility, fracture stiffness, and resistance to infinitesimally small stresses of a given material. The bulk modulus exhibits a positive correlation with the material's stiffness and its capacity to resist volume reduction. Specifically, an increased degree of resistance to volume reduction and increased rigidity contribute to a larger bulk modulus. UO's bulk modulus has been determined to be 206 GPa. By comparing this value to the mass moduli of other materials, such as glass and diamond, which range from 35-50 GPa and 443 GPa, respectively, it can be concluded that UO falls within the category of hard materials. The shear modulus (*G*) is defined as the proportionality between the applied shear force and the observed shear strain.

Stated differently, the shear modulus is a measure of a material's ability to withstand reversible deformations. A greater capacity to resist plastic deformation is indicative of a higher shear modulus. According to our estimation, the UO compound's shear modulus is approximately 58GPa. Young's modulus (*Y*) refers to the ratio of uniaxial pressure to longitudinal changes. The magnitude of the Y parameter in a material is directly proportional to its stiffness and exhibits greater resistance to plastic deformation. According to the results obtained from the optimized lattice constant, Young's modulus of UO has been estimated to be approximately 158 GPa. This classification implies that UO can be categorized as a stiff material. The Poisson's ratio (*v*) may serve as a valuable tool in elucidating chemical bonding properties, plastic behavior, and interatomic forces of a material. The contraction stress ratio to tensile strain, denoted by *v*, arises when a crystal experiences stretching pressure. The present study reveals that the values of ionic bonds fall within the range of 0.25-0.5, whereas metallic and covalent bonds exhibit values of 0.33 and 0.1 when the material exhibits maximum and minimum limits of 0. 255 of *v*, correspondingly, the fundamental properties of interatomic forces become significant. Table 2 presents a conspicuous outcome whereby the estimated v value for UO is recorded as 0.36. This indicates that the material characterizes an ionic bonding configuration, where interatomic forces exhibit a central nature. The authors have posited the existence of an empirical ratio referred to as Pugh's index [26] as a predictive tool for determining a material's propensity towards ductility or brittleness. The aforementioned criterion distinguishes materials with brittle characteristics from their ductile counterparts, and this distinction is dependent on a critical value of 1.75. The present study finds that ductility exhibits a *B/G* ratio greater than 1.75 (2.79 for aluminum), while brittleness exhibits a *B/G* ratio lower than 1. 75 (0.8 for diamonds). Based on the findings presented in Table 2, the amount of UO has been estimated to be approximately 3.5, which suggests that this particular compound possesses ductility. Table 3 presents the quantitative values of Vickers hardness (H_v), Zener's anisotropy factor (A^Z), universal anisotropy (A^U), Kleinmann parameter (ζ) , and Lamés' coefficients (μ, λ). The Kleinmann parameter is a noteworthy mechanical parameter that characterizes the relative arrangements of

anions and cations within a sublattice amidst strain-induced distortions while preserving volume. Furthermore, this parameter elucidates the inherent characteristics of a material's intermolecular bonds, encompassing stretching and bending dynamics. The Kleinmann parameter exhibits a range of values that span from 0 to 1 inclusively ($0 \leq \zeta \leq 1$), where the lower and upper bounds correspond to the minimum and maximum values, respectively. The obtained value of ζ is estimated to be around 0.40, indicating that bond-bending mechanisms exert more influence on these bonds compared to bond-stretching mechanisms. The utilization of Zener's anisotropy factor (A^z) and universal anisotropy (A^U) can serve as a means of assessing the anisotropic characteristics of materials in a more comprehensive manner. If the A^Z value tends towards unity, the substance exhibits isotropic characteristics. Conversely, if the A^Z value differs from unity, the material is regarded as exhibiting anisotropic properties. The estimation of the A^Z value for the substance UO yields a value of 0.17, signifying the anisotropic nature of UO. Furthermore, the value of zero for A^U serves as an indicator of the crystal's isotropy, while any deviation from this value suggests the presence of anisotropy. The observation of larger values for A^U indicates a heightened level of anisotropy within the material. With respect to UO, a numerical value of 4.5 has been computed, thereby corroborating the anisotropic nature of this particular compound. The determination of the three-dimensional (3D) surface constructions pertaining to the linear compressibility, shear modulus, Young's modulus, and Poisson's ratio [22] is a useful approach for the enhanced assessment of elastic anisotropy. If the three-dimensional surface representation indicates a spherical shape, the substance exhibits isotropic properties. In the interim, divergence from the spherical surface serves as an indication of the extent of anisotropy present within a given substance. Figure 3(a) depicts a tridimensional plot that showcases the linear compressibility (*1/B*) properties of the UO compound. As demonstrated, the aforementioned parameter exhibits a spherical morphology, implying the isotropic nature of the bulk modulus. The three-dimensional surface representations of the reciprocal values of *G* and *Y*, as well as the Poisson's ratio, are depicted in Figures 3 (b)-(d). The figures in question suggest that there exists a departure from sphericity, which consequently demonstrates elastic anisotropy in UO. All parameters derived from equations (9) and (10) have been computed and are presented in Table 4. The Debye temperature (Θ_D) obtained through the use of the average sound velocity yields a value of approximately 253 K. Additionally, the compressional (υ_l), shear (υ_s), and average (υ_m) velocities of sound for UO compound have been computed to be 4373 m/s, 1978 m/s, and 3729 m/s, respectively.

Table 2. Calculated elastic stiffnesses bulk modulus, shear modulus, Young's modulus (B_H, G_H, Y/GPa), Pugh's index (B/G), Poisson's ratio (υ) and (C_{ij}/GPa).

	C_{11}	C_{12}	C_{44}	B_H	G_H	Y	ν	B/G
UO	408	106	26	206	58	158	0.36	3.5

Table 3. Calculated Vickers hardness (H_V in GPa), Zener's anisotropy factor (A^Z), universal anisotropy (A^U), Kleinman parameter (ζ), and Lamés' coefficients (μ, λ) for UO.

	H_V^B	H_V^G	H_V^Y	A^Z	A^U	ζ	μ	λ
UO	19.83	8.55	9.60	0.17	4.5	0.40	58.08	149.68

Table 4. Calculated sound velocities, melting point, Debye temperature (Θ_D) and density.

	$\rho\left(\frac{g}{cm^3}\right)$	$V_l\left(\frac{m}{s}\right)$	$V_S\left(\frac{m}{s}\right)$	$V_m\left(\frac{m}{s}\right)$	$\theta_D(K)$	$T_m(K)$
UO	14.8	4373	1978	3729	253	2964 ± 300

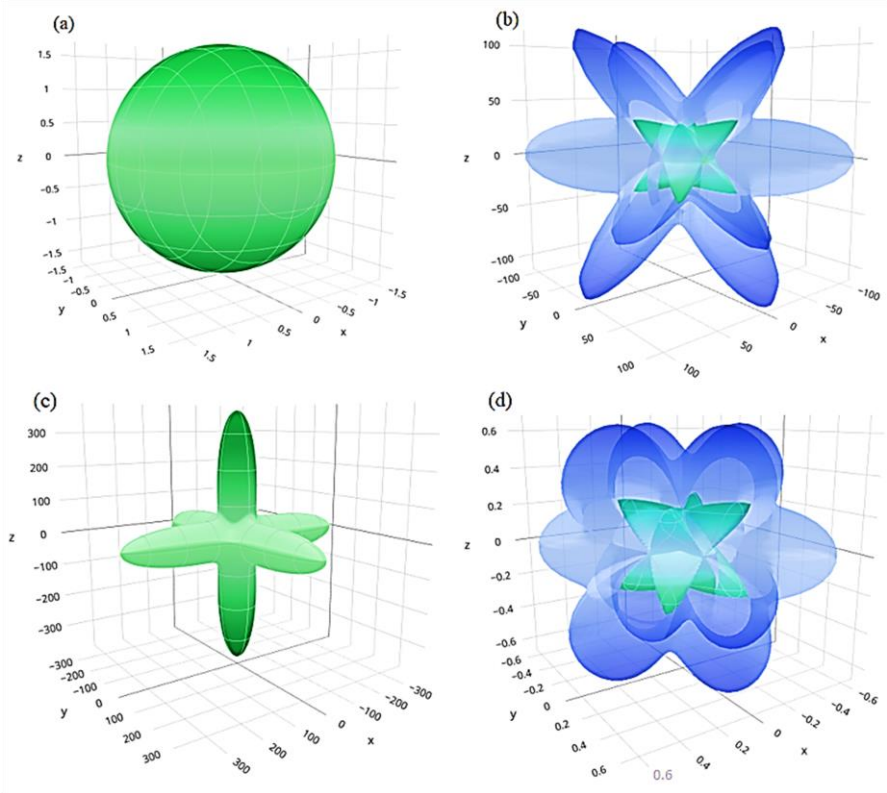

Fig. 3. 3D graph constructions of **a.** liner compressibility, **b.** shear modulus, **c.** Young's modulus, **d.** and Poisson's ratio of UO.

4.3. Phonon properties

Phonons are discrete quanta of vibrational energy that exist within a regular crystal lattice and propagate at sound velocity [27-30]. The phonon dispersion relationships elucidatepertinent physical occurrences, including but not limited to Umklapp scattering and the velocity of elastic waves. The phonon dispersion for uranium monoxide is computed assuming a cubic lattice structure and illustrated in Figure 4. The selection of the phonon spectrum is based on the utilization of the high symmetric directions within the first Brillouin region. The origin of the six phonon branches observed in the dispersion relations, namely three acoustic branches and three optical branches, can be attributed to the presence of two distinct atoms in the primitive unit cell of UO. This phenomenon can be understood from an academic perspective. Furthermore, the acoustical oscillations, which reside within the low-frequency spectrum, exhibit two transverse acoustical (TA) modes and one longitudinal acoustical (LA) mode. In contrast, within the upper-frequency region, the optical branches exhibit a configuration featuring a pair of transverse optical (TO) modes and a singular longitudinal optical (LO) mode. The present diagram depicts the dual degeneracy of the TA branch along the path from Γ to X. Additionally, a degeneracy within the TO branch has been observed in the direction from Γ →X, then removed, and observed again in the Γ→L direction. The fundamental criterion for dynamic stability is the absence of imaginary frequencies in the phonon dispersion. As illustrated in the aforementioned diagram, the non-negative phonon frequencies provide evidence for the dynamical stability of the crystal. Figure 5 depicts the vibrational density of states (VDOS), which has been utilized for the purpose of thorough examination and analysis of the phonon dispersion

curve. Due to the disparate masses of uranium and oxygen atoms, the vibrational density of states (VDOS) can be partitioned into distinct areas. Specifically, the relatively lighter oxygen atoms generate a higher degree of displacement, which in turn governs the optical frequencies within the range of 354-422cm^{-1}, primarily reflecting activity on the O surface. Conversely, the acoustic modes within the range of 0-141 cm^{-1}, primarily originating from uranium vibrations, exhibit a dominant influence on the VDOS. In solid-state physics, the concept of the Einstein frequency (ν_E) pertains to a collection of distinct oscillators that exhibit identical optical modes. Based on the data presented in Figure 5, it has been determined that the apex of the vibrational density of states (VDOS) curve, referred toas ν_E and located at the Γ point, possesses a calculated value of 369 cm^{-1} (11.06 THz). This result is deemed to be consistent with the value of 10.95 THz previously obtained through inelasticneutron scattering, as delineated in a previous study [8]. However, it should be noted that the UO compound exhibits a band gap between141-354 cm^{-1}. Within this spectrum, electromagnetic waves are substantially attenuated and lack the ability to propagate within the given medium, leading to complete reflection from the surface.

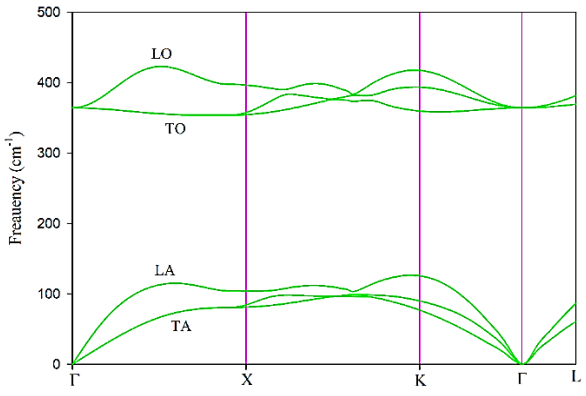

Fig. 4. Calculated phonon spectrum at zero pressure.

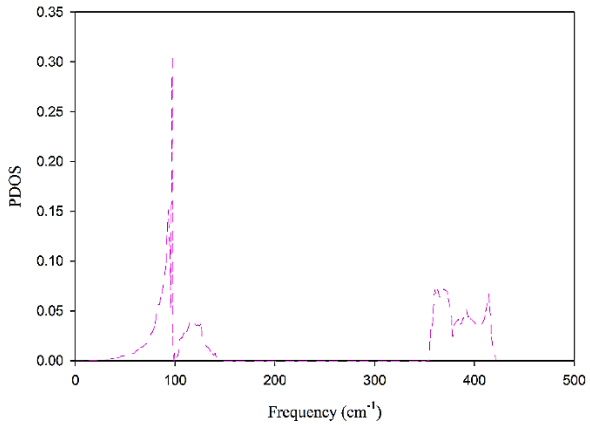

Fig. 5. Phonon density of states at equilibrium conditions.

5. Conclusions

The vibrational, thermophysical, elastic, and mechanical properties of UO nuclear fuel have been investigated using ab initio method and density functional theory.To summarize, results obtained from the aforementioned techniques are presented herein. The findings of the study indicate a satisfactory level of agreement between the obtained lattice constant under zero pressure. The estimated coefficients display a positive orientation and fulfill the Born-Huang equation, which indicates compound mechanical stability. The present study aimed to determine UO elastic moduli, such as shear modulus, bulk modulus, and Young's modulus. Findings from the analysis indicate UO's remarkable stiffness.The present study aimed to determine UO elastic moduli, such as shear modulus, bulk modulus, and Young's modulus. Findings from the analysis indicate UO's remarkable stiffness. The criterion proposed by Pugh, expressed as the ratio of bulk modulus to shear modulus (*B/G*), is found to be approximately 3.5, corroborating that the material under consideration, UO, exhibits ductility. The analysis of elasticity comprising both universal anisotropy and Zener's anisotropy factor reveals that the material under examination belongs to the class of

anisotropic materials. The phonon spectrum curve is determined via the Density Functional Perturbation Theory (DFPT) method by tracing the high symmetric paths. It is observed that there are no negative frequencies present in the dispersion relations. This observation indicates that the crystalline structure exhibits dynamic stability. There is a lack of experimental data on the effect of pressure/temperature on uranium oxide's elastic and phononic properties. As a suggestion, nuclear researchers can theoretically find the effects of different physical properties.

References

1. Sahafi MH, Akhavan O. Study on Structural, Dynamical, and Thermal Properties of Nuclear Fuel Thorium Mononitride Using First-Principles Calculations. JONSAT. 2024;45 (1):12-20. https://doi.org/10.24200/nst.2023.1242.1808
2. Baranov V, Devyatko YN, Tenishev A, Khlunov A, Khomyakov O. A physical model for evaluating uranium nitride specific heat. J. Nucl. Mater. 2013;434 (1-3):248-251. https://doi.org/10.1016/j.jnucmat.2012.10.047
3. Sanati M, Albers RC, Lookman T, Saxena A. Elastic constants, phonon density of states, and thermal properties of UO 2. Phys. Rev. B: Condens. Matter. 2011;84 (1):014116. https://doi.org/10.1103/PhysRevB.84.014116
4. Devey A. First principles calculation of the elastic constants and phonon modes of UO2 using GGA+ U with orbital occupancy control. J. Nucl. Mater. 2011;412 (3):301-307. https://doi.org/10.1016/j.jnucmat.2011.03.012
5. Brooks M. Electronic structure of NaCl-type compounds of the light actinides. II. Uranium monochalcogenides and monopnictides. J. Phys. F: Met. Phys. 1984;14 (3):653. https://doi.org/10.1088/0305-4608/14/3/010
6. Wedgwood F. Actinide chalcogenides and pnictides. III. Optical-phonon frequency determination in UX and ThX compounds by neutron scattering. J. Phys. C: Solid State Phys. 1974;7 (18):3203. https://doi.org/10.1088/0022-3719/7/18/006
7. Tougait O, Noël H. Stoichiometry of UAl4. Intermetallics. 2004;12 (2):219-223. https://doi.org/10.1016/j.intermet.2003.09.012
8. Chattaraj D, Majumder C. Structural, electronic, elastic, vibrational and thermodynamic properties of U3Si2: A comprehensive study using DFT. J. Alloys Compd. 2018;732 160-166. https://doi.org/10.1016/j.jallcom.2017.10.174
9. Wang B-T, Zhang P, Lizárraga R, Di Marco I, Eriksson O. Phonon spectrum, thermodynamic properties, and pressure-temperature phase diagram of uranium dioxide. Phys. Rev. B: Condens. Matter. 2013;88 (10):104107. https://doi.org/10.1103/PhysRevB.88.104107
10. Singh S, Gupta SK, Sonvane Y, Nekrasov K, Kupryazhkin AY, Gajjar P. Ab-initio calculation on electronic and optical properties of ThO2, UO2 and PuO2. J. Nucl. Mater. 2018;511 128-133. https://doi.org/10.1016/j.jnucmat.2018.08.055
11. Chen H. The mechanical and thermodynamic properties of α-Na3 (U0. 84 (2), Na0. 16 (2)) O4: A combined first-principles calculations and quasi-harmonic Debye model study. Nucl. Eng. Technol. 2021;53 (2):611-617. https://doi.org/10.1016/j.net.2020.07.027
12. Mehmetoglu T. Use of Einstein-Debye method in the analytical and semi empirical analysis of isobaric heat capacity and thermal conductivity of nuclear materials. J. Nucl. Mater. 2019;527 151827. https://doi.org/10.1016/j.jnucmat.2019.151827
13. Yamashita T, Nitani N, Tsuji T, Kato T. Thermal expansion of neptunium-uranium mixed oxides. J. Nucl. Mater. 1997;247 90-93. https://doi.org/10.1016/S0022-3115(97)00031-7
14. Giannozzi P, Baroni S, Bonini N, Calandra M, Car R, Cavazzoni C, Ceresoli D, Chiarotti GL, Cococcioni M, Dabo I. QUANTUM ESPRESSO: a modular and open-source software project for quantum simulations of materials. J. Phys.: Condens. Matter. 2009;21 (39):395502. https://doi.org/10.1088/0953-8984/21/39/395502

15. Pack JD, Monkhorst HJ. " Special points for Brillouin-zone integrations"—a reply. Phys. Rev. B: Condens. Matter. 1977;16 (4):1748. https://doi.org/10.1103/PhysRevB.16.1748

16. Kulik HJ, Cococcioni M, Scherlis DA, Marzari N. Density functional theory in transition-metal chemistry: A self-consistent Hubbard U approach. Phys. Rev. Lett. 2006;97 (10):103001. https://doi.org/10.1103/PhysRevLett.97.103001

17. Baroni S, Giannozzi P, Isaev E. Density-functional perturbation theory for quasi-harmonic calculations. Rev. Mineral. Geochem. 2010;71 (1):39-57. https://doi.org/10.1515/9781501508448-005

18. Pfrommer BG, Côté M, Louie SG, Cohen ML. Relaxation of crystals with the quasi-Newton method. J. Comput. Phys. 1997;131 (1):233-240. https://doi.org/10.1006/jcph.1996.5612

19. Dal Corso A. Elastic constants of beryllium: a first-principles investigation. J. Phys.: Condens. Matter. 2016;28 (7):075401. https://doi.org/10.1088/0953-8984/28/7/075401

20. Jamal M, Asadabadi SJ, Ahmad I, Aliabad HR. Elastic constants of cubic crystals. Comput. Mater. Sci. 2014;95 592-599. https://doi.org/10.1016/j.commatsci.2014.08.027

21. Wu Z-j, Zhao E-j, Xiang H-p, Hao X-f, Liu X-j, Meng J. Crystal structures and elastic properties of superhard Ir N 2 and Ir N 3 from first principles. Phys. Rev. B: Condens. Matter. 2007;76 (5):054115. https://doi.org/10.1103/PhysRevB.76.054115

22. Sahafi M, Mahdavi M. First principles study on phonon dispersion, mechanical and thermodynamic properties of ThP. Mater. Today Commun. 2021;26 101951. https://doi.org/10.1016/j.mtcomm.2020.101951

23. Sahafi M, Mahdavi M. Ab initio investigations on lattice dynamics and thermal characteristics of ThO2 using Debye–Einstein model. Bull. Mater. Sci. 2021;44 (2):1-9. https://doi.org/10.1007/s12034-021-02370-0

24. Sahafi M. First-principles investigation of phonon spectrum, elastic, mechanical and thermophysical characteristics of an actinide-oxide ceramic. J. Solid State Chem. 2023;124102. https://doi.org/10.1016/j.jssc.2023.124102

25. Birch F. Finite strain isotherm and velocities for single-crystal and polycrystalline NaCl at high pressures and 300 K. J. Geophys. Res.: Solid Earth. 1978;83 (B3):1257-1268. https://doi.org/10.1029/JB083iB03p01257

26. Pugh S. XCII. Relations between the elastic moduli and the plastic properties of polycrystalline pure metals. The London, Edinburgh, and Dublin Philosophical Magazine and Journal of Science. 1954;45 (367):823-843. https://doi.org/10.1080/14786440808520496

27. Sahafi M, Mahdavi M. Ab-initio investigations on dynamical and lattice thermal behaviours of ThC. Bull. Mater. Sci. 2021;44 (2):98. https://doi.org/10.1007/s12034-021-02371-z

28. Sahafi MH, Akhavan O. Study of Temperature and Pressure Effect on Thermodynamic Properties of Thorium Phosphide Compound. Iranian Journal of Applied Physics. 2023;7-24. https://doi.org/10.22051/ijap.2023.42680.1312

29. Sahafi MH, Mahdavi M. Theoretical study of ThO2 by first principles calculations. Iranian Journal of Physics Research. 2021;21 (1):91-109. https://doi.org/10.47176/ijpr.21.1.41038

30. Sahafi MH, Mahdavi M. Investigation of Vibrational and Thermodynamic Characteristics of ThC Under High Pressure and Temperature. Journal of Research on Many- body Systems. 2022;12 (2):49-62. https://doi.org/10.22055/jrmbs.2022.17627.

How to cite this article

M. H. Sahafi, E. Cholaki, *Ab Initio Study of Mechanical and Vibrational Characteristics of Uranium Monoxide in Nuclear Reactor*, Journal of Nuclear Science and Applications (JONRA), Vol. **3,** No. **4,** P **1-11,** Autumn **(2023), Url**: https://jonra.nstri.ir/article_1606.html**, DOI**: https://doi.org/10.24200/jon.2023.1070.